CCE 2020

CCE

2020, 17th International Conference on Electrical Engineering, Computing Science and Automatic Control

Mexico City, Mexico.
November 11-13, 2020

CALL FOR PAPERS

The main goal of CCE is to provide a forum for free discussion and interchange of research and development experiences and ideas, in the fields of electrical-electronics engineering, computer science and automatic control.

This conference also offers an opportunity for younger researchers and students to meet more experienced colleagues from differents parts of the world. Conference content will be submitted for inclusion into IEEE Xplore as well as other Abstracting and Indexing (A&I) databases.

Submitted manuscripts should be six (6) pages or four (4) pages in IEEE two-column format, including figures, tables, and references.

General Chairs

Dr. Gerardo Silva Navarro
Dr. Wen Yu Liu
Dr. Sergio Salazar Cruz

Information

Address: Av. Instituto Politécnico Nacional 2508, Col San Pedro Zacatenco,
Alcaldía Gustavo A. Madero
City: Mexico City
Country: Mexico
CP: 07360
Phone: +52 (55) 5747-3800 Ext 6503
FAX: +52 (55) 5747-3976
cce@cinvestav.mx

In support of the health contingency due to COVID19, registration costs has been reduced

Deadline

Full Manuscript: July 6, 2020 extended to August 14, 2020
Review Notification (Phase 1): Before September 4, 2020
Final Revised Manuscript: September 18, 2020
Verification of final manuscript and Papers accepted (Phase 2): September 28, 2020
Submit Payment (Authors): October 12, 2020

Topics

Include but not limited to:

- Automatic Control
- Computer science and computer engineering
- Biomedical engineering
- Communications systems
- Mechatronics
- Mechanical Engineering
- Aeronautic and Aerospace Engineering
- Solid-state materials, electron devices and integrated circuits
- Power Electronics
- Nanotechnology (materials and applications)
- Autonomous Navigation
- Exoskeletons

http://cce.cinvestav.mx

ISSN
Online: 2642-3766

ISBN
978-1-7281-8987-1

IEEE
Electron Devices Society
Cinvestav

Proposal for a rotary micromotor structure based on CMOS-MEMS technology

Luis Sánchez-Márquez, Mario Alfredo Reyes-Barranca,
Electrical Engineering Dept.
CINVESTAV-IPN
Mexico City, Mexico
{luis.sanchez.m, mreyes} @cinvestav.mx

Griselda Stephany Abarca-Jiménez
UNIDAD PROFESIONAL INTERDISCIPLINARIA EN INGENIERIA CAMPUS HIDALGO INSTITUTO POLITÉCNICO NACIONAL
Hidalgo, 42162,Mexico
gabarcaj@ipn.mx

Andrea López-Tapia, Luis Martín Flores-Nava
Electrical Engineering Dept.
CINVESTAV-IPN
Mexico City, Mexico
{andrea.lopez, lmflores} @cinvestav.mx

***Abstract*— This paper shows a design proposal for a MEMS rotary micromotor based on the design rules of the 0.5 micron CMOS technology of On Semiconductor. With simulations carried out in COMSOL, the electrostatic behavior of the proposed micromotor is shown; the simulation helps us to know the maximum friction force that our design is capable of overcoming when the micromotor is powered with 18 volts.**

***Keywords*— MEMS, micromotor, CMOS technology.**

I. Introduction

Some works [1] [2] [3] [4] [5] talk about the design of rotary micromotors manufactured using CMOS technology or technologies dedicated to the manufacturing of MEMS (such as MEMSCAP [6] [7]); the dedicated technologies have specific layers for manufacturing each part of a micromotor, as can be seen in [3].

The 0.5 micron CMOS technology of On Semiconductor [8] is not intended to make MEMS devices. The novelty of this work is that it proposes the most suitable layers for the manufacture of a low voltage rotary micromotor considering the design rules of the 0.5 micron CMOS technology of On Semiconductor; that is, it is the first micromotor designed with this technology. In addition, this micromotor will be integrated into a single chip together with the control electronics and a speed sensor [9], however this work only focuses on the proposal of the micromotor structure.

A. Micromotors review

Micromotors are devices that generate a movement due to some micro-acting force (primarily electrostatic forces). The force generated in parallel pairs of misaligned and electrically energized plates stimulates the movement required in a micromotor [10].

Fig. 1 shows a schematic of a rotary micromotor, the rotor and stator are made of a conductive material. The stator poles are connected in an alternating sequence of three electrical phases (φ_1 is connected to E1, φ_2 is connected to E2 and φ_3 is connected to E3) and by applying a potential difference (control voltage) with a specific minimum value to the misaligned poles, an electrostatic force is generated between them which causes the rotor to rotate one step; if this is done in an appropriate sequence and periodically the rotor can be rotated at a certain speed in a clockwise or counterclockwise direction [10].

The cross section of Fig. 2 shows the main parts that make up a rotary electrostatic micromotor [3]. The entire structure is made of some conductive material. The bushings serve both as electrical contact (to supply the rotor) and mechanical contact.

Since the bushings are in contact with the base, it is necessary to overcome the friction force present between the rotor and the base for the rotor to rotate. The electrostatic force between the rotor and stator poles is responsible for overcoming the friction force, therefore the control voltage must be large enough to generate that electrostatic force.

The most important geometric parameters in the design of a micromotor are the following: Number of rotor poles (N_r), number of stator poles (N_s), rotor radius (r_o), rotor poles height (Δr), shape of rotor poles, shaft radius (r_{sh}), gap between rotor and stator poles (d), shaft-rotor gap (r_{er}), rotor thickness (t), base radius (r_{base}) and bushings diameter (d_c) (see Fig. 3).

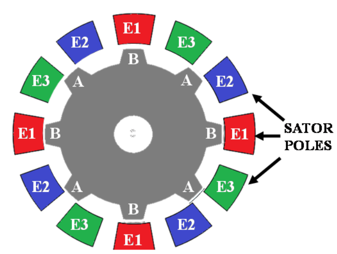

Fig. 1. Schematic of a rotary micromotor

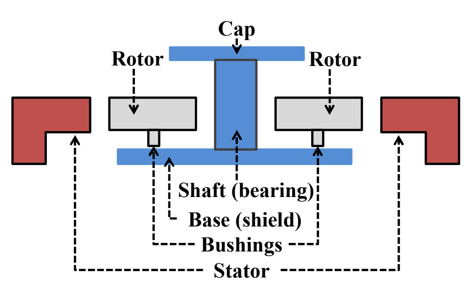

Fig. 2. Schematic of the cross section of the parts that make up a micromotor

978-1-7281-8987-1/20/$31.00 ©2020 IEEE

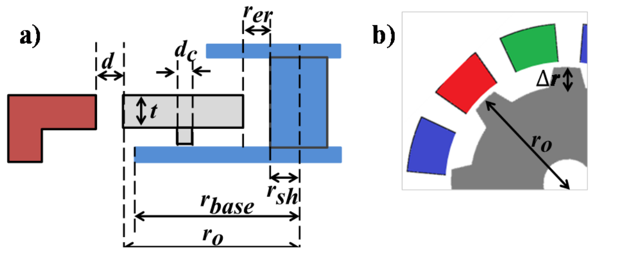

Fig. 3. Schematic of a portion of the micromotor and its geometric parameters (a) cross section (b) plan view

It is possible to design a micromotor that works with small control voltages (below 20 V) if these geometric parameters are appropriately selected.

B. Friction in microstructures

In the macro scale the friction force is proportional to the weight W ($F = \mu W$) and the coefficient of friction μ is independent of both the weight and the contact area. However, in the micro scale the behavior of friction forces changes [11].

The experimental results using microstructures indicate that the friction coefficients are affected by normal loads (the friction coefficient decreases with the normal load), the crystal orientation and the manufacturing processes of the samples [11].

The 0.5 micron CMOS technology has two polysilicon layers [8]. As will be seen later, one of these layers is used for the manufacture of the micromotor.

Some values of the friction coefficient (for polysilicon) are reported in [11], ranging from $\mu = 0.7 \pm 0.3$ to values as high as 7.8. The dispersion of the friction coefficients in MEMS devices is also attributed to microscopic debris located on surfaces and between microstructures.

That is, in the micro scale, the friction coefficient is affected by different factors, hence each particular case can present its friction coefficient value. Therefore, in this work, the friction coefficient will be considered as a variable when designing the micromotor structure.

II. Design of the Micromotor Structure

To move the micromotor, a minimum control voltage must be applied to overcome the friction force produced by the friction of the bushings with the turning base.

The friction force is given by (1), where μ is the friction coefficient, g =9.81m/s^2, W_o is the weight of the rotor and m is the mass of the rotor, given by (2).

$$F_f = \mu W_o = \mu m g \quad (1)$$

$$m = \rho Vol \quad (2)$$

Where Vol is the volume of the rotor and ρ is the density of the material.

Fig. 4 shows a schematic of the proposed structure for the micromotor. In order to know the volume, some geometric parameters are defined (in addition to those previously defined in Fig. 3):

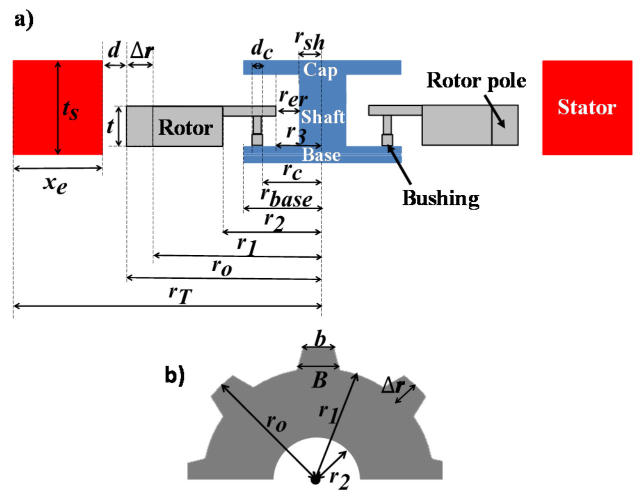

Fig. 4. (a) Cross section (schematic) of the micromotor and its geometric parameters (b) Parameters that define the shape of the rotor of the micromotor

The thickness of the stator (t_s), length of the stator poles (x_e); the total radius of the micromotor (r_T); distance between the center of the shaft and the beginning of the bushings (r_c); r_3 is the distance between the center of the shaft and the start of the rotor and is given by $r_3 = r_{er} + r_{sh}$; B and b are the bases of the trapezoid that forms the rotor poles; r_1 and r_2 are defined since the section of the rotor that is between these radiuses will be used to place a capacitor plate that will serve as a speed sensor (this is mentioned only to justify these parameters, for more details of the speed sensor see [9]).

Sectioning the rotor into three parts, as shown in Fig. 5, we obtain that the total volume is approx. $Vol \approx (A1+N_r A2)t+A3t_o$. Where t_o is the thickness of the rotor until before reaching r_2.

$$Vol = \left[\pi\left(r_1^2 - r_2^2\right)+N_r\left(\Delta r\frac{B+b}{2}\right)\right]t+\left[\pi\left(r_2^2 - r_3^2\right)\right]t_o \quad (3)$$

From (1), (2) and (3) we obtain that the friction force is given by

$$F_f = \mu g \rho\left\{t\left[\pi\left(r_1^2 - r_2^2\right)+N_r\Delta r\frac{B+b}{2}\right]+t_o\left[\pi\left(r_2^2 - r_3^2\right)\right]\right\} \quad (4)$$

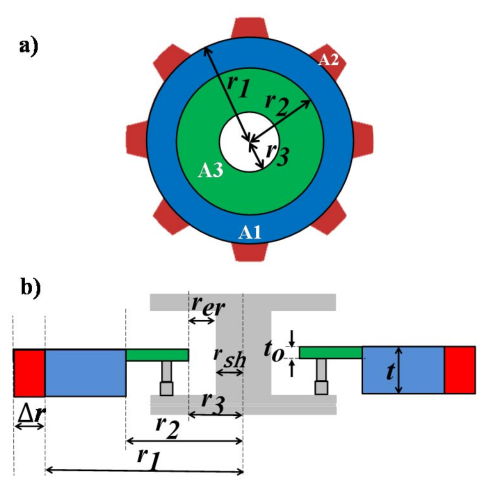

Fig. 5. Rotor structure divided into three sections; A1 and A3 in the form of a flat ring and A2 in the form of a trapezoid. (a) Plan view (b) cross section

In order to obtain the electrostatic actuation force present in the micromotor, given by (5), is used the principle of operation of a misaligned parallel plates actuator [7] [12]. Where ε_a is the permittivity of air, N is the number of pair of poles that are activated at the same time and V_o is the control voltage.

$$F_e = N\varepsilon_a \frac{t}{2d} V_o^2 \tag{5}$$

If a ratio of number of rotor and stator poles of 2:3 is used, i.e. N_r/N_s =2/3, the number of poles N that generate the force is given by

$$N = \frac{N_r}{2} \tag{6}$$

In order to overcome the friction force, the inequality $F_e > F_f$ must be satisfied; from (5) and (6) we obtain that the minimum control voltage generated by an F_e capable of defeating F_f is

$$V_{o_{min}} = \sqrt{\frac{4F_f\, d}{\varepsilon_a\, N_r\, t}} \tag{7}$$

A. Selection of the materials that make up the structure

The 0.5 micron CMOS technology of On Semiconductor features three layers of metal and two layers of polysilicon of different thicknesses. The layers are separated by silicon oxide of different thicknesses (for more details see [7]). The layers can be electrically connected through metal contacts (see the schematic in the Fig. 6).

Fig. 7 shows a schematic of the cross section of the proposed structure for the micromotor. It is observed that after the release of the rotor (removal of silicon oxide [13]), it falls and makes contact with the base through the bushings.

In (5) it can be seen that the actuation force strongly depends on the thickness of the rotor t, therefore it was decided to manufacture the rotor structure using the Metal1 and Metal2 layers. The thicknesses of these metals are, respectively: $TM1$=0.64µm; $TM2$=0.57µm [8]. These metals are joined by means of metal contacts with a thickness of $TVIA1$=1.1µm, Hence the rotor thickness is $t = TM1+TM2+TVIA1$=2.31µm.

The Metal3 layer available in On-Semi technology has a thickness greater than Metal1 and Metal2 ($TM3$ = 0.77µm), however Metal3 is used to build a shaft cap [1].

In order to form the stator structure, Metal2, Metal1 and Poly2 layers are used, joined by means of metal contacts. So the thickness of the stator poles is $t_s = TM2+TVIA1+TM1+P2CNT+TPOLY$.

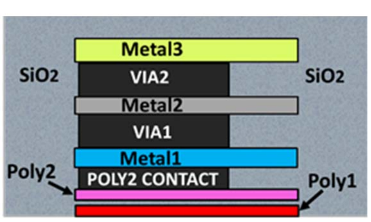

Fig. 6. Schematic of the layers available in On Semiconductor 0.5 micron technology

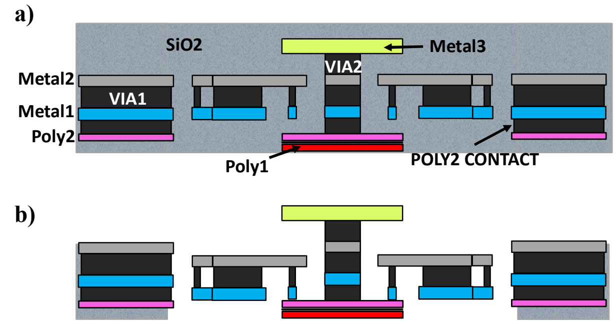

Fig. 7. Schematic of micromotor cross section with On-Semi 0.5 micron CMOS technology layers (a) before rotor release (b) after rotor release

Where $P2CNT$=0.747µm is the thickness of the contact that joins Poly2 and Metal1; $TPOLY$=0.35µm is the thickness of Poly2 [8]. Therefore t_s=3.407µm.

B. Considerations to define the geometric parameters of the micromotor

The considerations presented below refer to Fig. 4, unless otherwise indicated.

An area of 500µm x 500µm is assigned for the micromotor structure, therefore it must be observed that $r_o+d+x_e \leq 250$ µm.

The value of the gap d is closely related to r_{er}. Suppose the micromotor is energized (there is a potential difference, V_o, between the rotor and stator) and, while rotating, the rotor is off-center. If $d < r_{er}$, the rotor will make contact with the stator producing a short circuit (see Fig. 8 (c) and (d)). On the other hand if $d > r_{er}$, contact is made between the rotor and the shaft; this would cause wear on the structure, but short circuit is avoided (see Fig. 9 (c) and (d)), so the design must satisfy the condition $d > r_{er}$.

Finally the parameter r_{er} must be large enough so that the rotor can be completely released during the micromachining [1]. Therefore the parameter $r_{er\,min}$=10λ is defined, where λ is the scaling factor of the device dimensions (λ is equal to 0.3µm in the 0.5µm technology), so $r_{er\,min}$=3µm.

In (5) it can be seen that in order to have a large actuation force with a small control voltage, the gap d must be as small as possible. A gap value d =12λ is proposed. This satisfies the condition $d > r_{er}$.

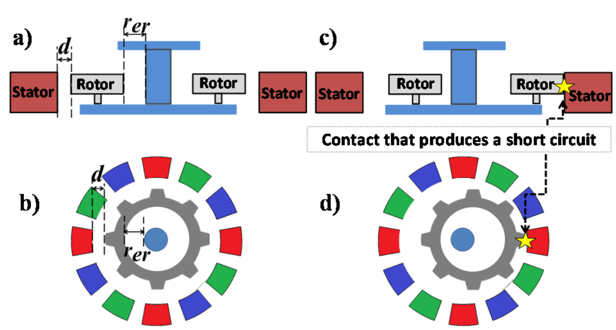

Fig. 8. Schematic of the micromotor when $d < r_{er}$. (a) Cross section of the centered rotor, (b) plan view of the centered rotor, (c) cross section of the off-center rotor, (d) plan view of the off-center rotor

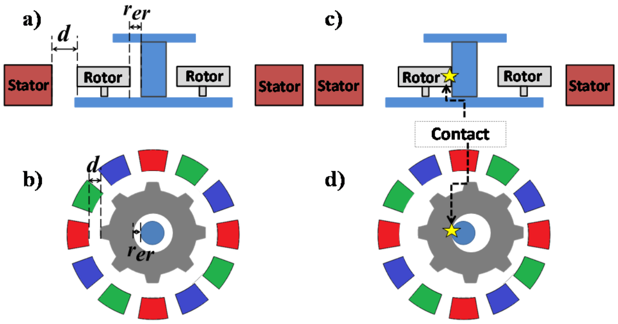

Fig. 9. Schematic of the micromotor when $d > r_{er}$. (a) Cross section of the centered rotor, (b) plan view of the centered rotor, (c) cross section of the off-center rotor, (d) plan view of the off-center rotor

Proposing r_1 =200µm and Δr=18µm (in this work the influence of the rotor poles shape is not studied, so this last parameter should be studied in future works), then r_o=218µm (see Fig. 4). It was said that $r_o+d+x_e \leq 250\mu m$, therefore $x_{e\ max}$=28.4µm.

On the other hand, if r_{sh} parameter is very small, the shaft could break due to the continuous friction that may exist with the rotor. The shaft radius is defined with a minimum value of $r_{sh\ min}$=50µm.

Fig. 4(a) shows that $r_c > r_{er} + r_{sh}$ must be satisfied, so a minimum value of $r_{c\ min}$=53µm is defined.

On the other hand, the bushings should be as small as possible (if the rotor-base contact area decreases, the value of µ will also decrease [11]). Therefore, using the minimum dimensions for the VIA1 layer of the 0.5µm technology [8], $d_{c\ min}$=4λ=1.2µm is defined.

Furthermore, the bushings must always be mounted on the base (even if the rotor is off-center), so the radius of the base must have a minimum value of $r_{base\ min}= r_c+d_c+r_{er}$, that is, $r_{base\ min}$= 57.2µm.

If the rotor is off-center, it must be ensured that only the bushings make contact with the base, so it must be satisfied that $r_2>r_{base}+r_{er}$, that is, $r_{2\ min}$= 63.2µm.

Table I summarizes the minimum and maximum dimensions for the micromotor structure.

C. Definition of the geometric parameters of the micromotor

Using the dimensions shown in Table I and t=2.31µm, t_o=0.57µm, ρ=2700 Kg/m^3 (density of Metal1 and Metal2), N_r=50, r_2=100µm, B=15µm, b=9µm, Δr=18µm and by varying the parameters µ, t, N_r, d, and r_2 in (4) and (7), the graphs of friction force F_f and minimum control voltage necessary to overcome the friction force $V_{o_{min}}$ are obtained.

Since there is no data on the coefficient of friction between Metal1 and Poly2, µ is taken as a parameter with values between 0.5 and 3 (although there was a reported value of µ, the measurements of the coefficient of friction in the micro scale are very scattered [11] [14], therefore cannot be assigned a specific value).

TABLE I. SUMMARY OF MAXIMUM AND MINIMUM DIMENSIONS FOR THE MICROMOTOR STRUCTURE

Parameter	Value	Parameter	Value	Parameter	Value
$r_{o\ máx}$	218µm	$r_{er\ min}$	3µm	$r_{c\ min}$	53µm
$r_{1\ máx}$	200µm	$r_{sh\ min}$	50µm	$r_{base\ min}$	57.2µm
$d_{mín}$	3.6µm	$d_{c\ min}$	1.2µm	$r_{2\ min}$	63.2µm

Fig. 10 shows the graphs of F_f and $V_{o_{min}}$ against rotor thickness t. It is observed that $V_{o_{min}}$ decreases as the rotor thickness increases; e.g. with µ=1 it is possible to decrease one volt with a greater thickness and almost two volts for µ=3.

The gap d is a very important geometric parameter since it does not modify the friction force (see (4)). Fig. 11 shows the graph of $V_{o_{min}}$ against the gap d. It is observed that when the gap becomes small, $V_{o_{min}}$ decreases considerably. Therefore, for the design of the structure, the minimum value of the gap mentioned above is selected (d = 3.6µm).

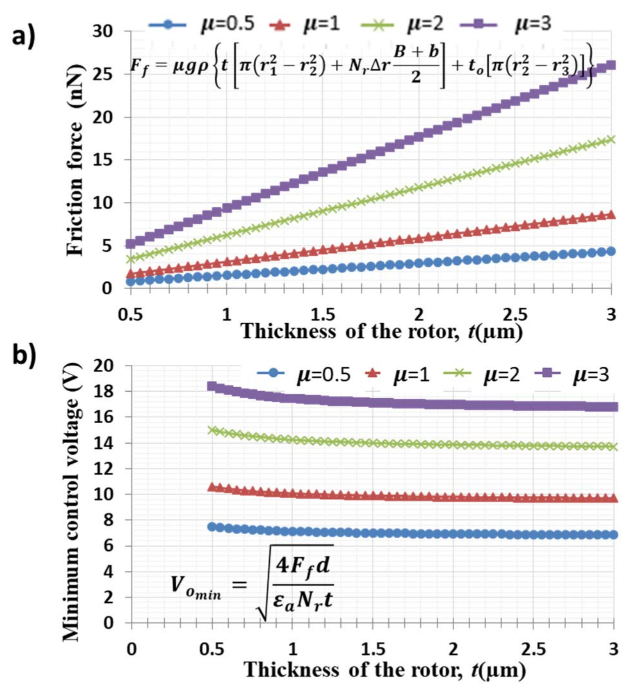

Fig. 10. (a) Friction force vs. rotor thickness (b) Control voltage vs. rotor thickness. In both graphs, a parametric sweep of µ is made.

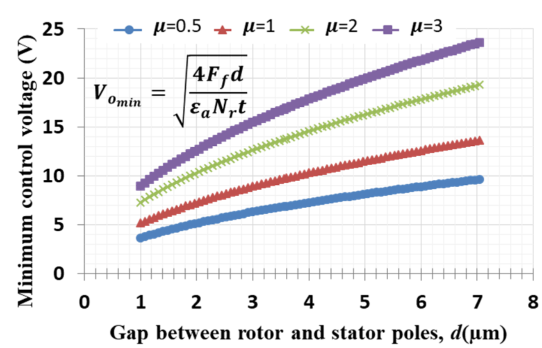

Fig. 11. Control voltage vs. gap between rotor and stator poles. In both graphs, a parametric sweep of µ is made.

Fig. 12 shows the graphs of F_f and $V_{o_{min}}$ against the number of rotor poles N_r. It is observed that when the number of the rotor poles is increased, the friction force increases. However, it is necessary to increase N_r, in order to considerably decrease the value of $V_{o_{min}}$. A value of N_r=50 is selected for the micromotor structure. It was said that N_r/N_s =2/3, therefore the number of stator poles is N_s=75.

If a greater number of rotor poles were selected, they must be of a smaller width, and the separation between each stator electrode would decrease, and the 0.5µm CMOS technology design rules could be violated. These rules specify the minimum dimensions of the layers and the minimum separation between two structures of the same material [8].

Fig. 13 shows the graphs of F_f and $V_{o_{min}}$ against r_2. It is observed that F_f and $V_{o_{min}}$ decrease when r_2 increases; having a decrease of eight volts when µ=3. Therefore, the geometric parameter r_2 must be as large as possible. This parameter can have a maximum value of 200µm ($r_2 = r_1$ see Fig. 4), but a value of r_2=180µm is chosen; it was mentioned that the section of the rotor that is between these radiuses will be used to place a capacitor plate that will serve as a speed sensor (for more details of the speed sensor see [9]).

Table II summarizes the geometric dimensions of the micromotor that have been defined based on the previous graphs. Substituting those values in (5) and (7) we have that the minimum control voltage to overcome the friction force is: $V_{o_{min}}$ =4.981V for µ=0.5; $V_{o_{min}}$ =7.045V for µ=1; $V_{o_{min}}$=9.963V for µ=2; $V_{o_{min}}$=12.203V for µ=3.

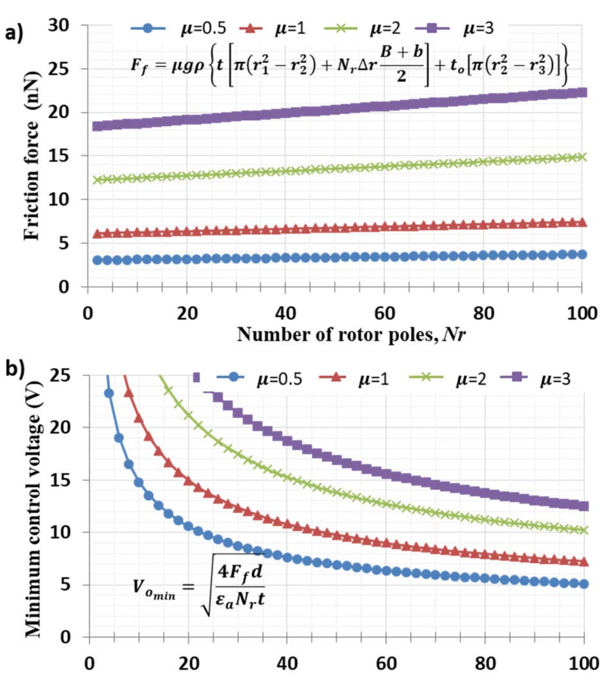

Fig. 12. (a) Friction force vs. number of rotor poles (b) Control voltage vs. number of rotor poles. In both graphs, a parametric sweep of µ is made.

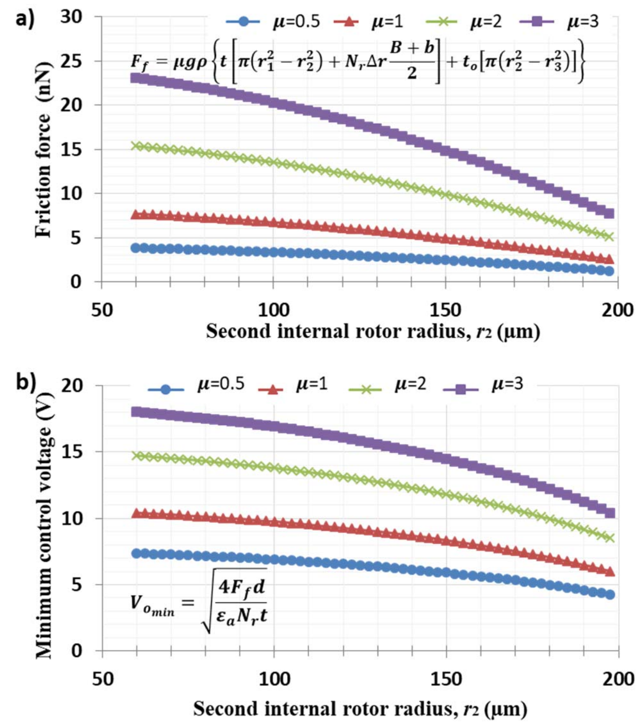

Fig. 13. (a) Friction force vs. second internal rotor radius (b) Control voltage vs. second internal rotor radius. In both graphs, a parametric sweep of µ is made.

III. RESULTS

To know the electrostatic behavior of the micromotor structure, a simulation is carried out in COMSOL, which implements the finite element analysis. The micromotor structure is drawn using the geometric parameters of Table II, however, in order to decrease the computation time, only the E2 electrodes (Fig. 1) of the micromotor structure are drawn.

A control voltage V_o = 18V is selected, since this overcomes the friction force for the different values of µ analyzed in the previous section. The electrostatic behavior of the micromotor is known by polarizing the rotor with V_o = 18V and the E2 electrodes with 0V.

Fig. 14 shows the result of the simulation. It is observed that the electric field intensity has a maximum value of 6MV/m. Fig. 15 shows a close up of the simulated structure. This shows the areas where the maximum value of the electric field is found (between the stator poles and the rotor B poles). This electric field generates the electrostatic force that causes the rotor to

TABLE II. GEOMETRIC DIMENSIONS FOR THE MICROMOTOR STRUCTURE

Parameter	Value	Parameter	Value	Parameter	Value
t	2.31µm	d	3.6µm	N_r	50
t_o	0.57µm	r_{base}	57.2µm	N_s	75
t_s	5.277µm	r_c	53µm	B	15µm
r_o	218µm	r_{er}	3µm	b	9µm
r_1	200µm	r_{sh}	50µm	Δr	18µm
r_2	180µm	d_c	1.2µm	x_e	20µm

rotate until its B poles align with the E2 poles of the stator. The value of the total electric force exerted by all the stator poles on the rotor is also shown (F_e=4.33nN). This is a small value compared to the expected value from (5) (F_e=22.998nN for a control voltage V_o= 18V).

This result is due to the fact that (5) is obtained from considering a pair of parallel plates whose separation is always constant [12]; however, the proposed shape of the rotor poles causes that there is no constant gap between them and the stator poles; in addition, as can be seen in Fig. 15, the A poles of the rotor also interact with the E2 poles of the stator, this causes a decrease in the attractive force between the B poles and the stator poles.

With F_e=4.33nN we could equal a friction force of the same value, F_e=F_f. Then, using (4), the coefficient of friction between the bushings and the motor base would be μ_{max}=1.228; that is, if a control voltage V_o=18V is applied, the micromotor proposed in this work will rotate as long as the coefficient of friction between the base and the bushings is less than 1.228.

IV. Conclusions

A rotary micromotor was designed based on the On Semiconductor 0.5 micron CMOS technology design rules; therefore the micromotor can be integrated together with the control electronics within the same chip.

The geometric parameters and the materials were selected in order to reduce both the control voltage and the friction force; the geometric parameters that define the rotor poles shape were also proposed, however a more detailed study of them is required to know their influence on the electrostatic behavior of the proposed micromotor structure.

The micromotor structure contemplates possible failures that can occur if the rotor becomes off-center while it is turning, such as preventing short circuits between the stator and the rotor. The short circuit can damage the structure or the control circuit inside the chip. These failures are prevented by selecting some geometric parameters appropriately.

The technology used does not have a special layer for the micromotor bushings manufacture; in this work, the way to construct the bushings using the Metal1 and Metal2 layers joined by means of a metallic contact was proposed.

The simulation results showed that for a control voltage of 18 volts, it is possible to overcome the friction force if the friction coefficient between the bushings and the base is less than 1.228.

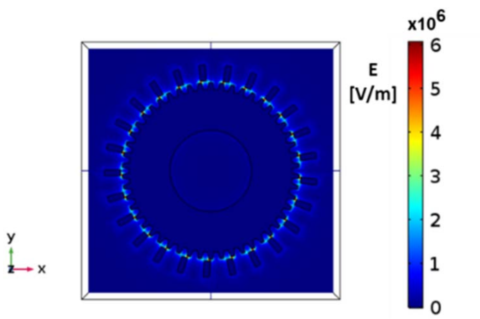

Fig. 14. Electric field distribution in the micromotor

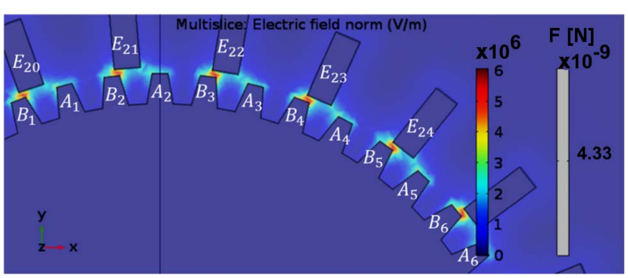

Fig. 15. Intensity of the electric field and magnitude of the electrostatic force.Close up to the structure of the micromotor

References

[1] J. Horstmann and K. Goser, "Monolithic integration of a silicon micromotor in combination with the CMOS drive circuit on one chip," 2003.

[2] M. A. Basha, S. Safavi-Naeini and S. K. Chaudhuri, "Design and fabrication of an electrostatic micromotor with a low operating voltage," pp. 1139-1142, Junio 2007.

[3] Dhananjay Barbade, Rohit Soni and Shriniwas Metan, Micromotor Fabrication by Surface Micromachining Technique, India, 2010.

[4] I. Dufourt, E. Sarraute and A. Abbas, "Optimization of the geometry of electrostatic micromotors using only analytical equations," *Journal of Micromechanics and Microengineering,* pp. 108-111, 1996.

[5] T. Kraus, M. Baltzer and E. Obermaider, "Design and fabrication of surface micromachined micromotors with large dimensions," pp. 196-199, 1997.

[6] MEMSCAP, 2011-2012. [Online]. Available: http://www.memscap.com/products/mumps/polymumps.

[7] M. Huff, Process Variations in Microsystems Manufacturing, Microsystems and Nanosystems. Springer, 2020.

[8] OnSemiconductor, C5X, 0.5 Micron Technology Design Rules, 2011.

[9] L. Sánchez-Márquez, M. A. Reyes-Barranca, G. S. Abarca-Jiménez, A. López-Tapia, L. M. Flores-Nava and O. Arellano-Cárdenas, Proposal of a speed sensor based on FGMOS for a MEMS rotatory micromotor, Mexico City: 16th International Conference on Electrical Engineering, Computing Science and Automatic Control (CCE), 2019.

[10] H. Tai-Ran, MEMS and microsystems : design and manufacture, McGraw-Hill, 2002.

[11] W. Wang, Y. Wang, H. Bao, B. Xiong and M. Bao, "Friction and wear properties in MEMS," *Elsevier Science,* pp. 486-491, Julio 2002.

[12] V. Kaajakari, Practical MEMS, Las Vegas: Small Gear Publishing, 2009.

[13] L. Sánchez-Márquez, Diseño y análisis de un micromotor angular basado en tecnología CMOS-MEMS, Mexico City: Master Thesis, CINVESTAV-IPN, 2018.

[14] W. Zhang, G. Meng and H. Li, "Electrostatic micromotor and its reliability," *Elsevier,* pp. 1230-1242, Abril 2005.